

Push & Pull: autonomous deployment of mobile sensors for a complete coverage

Novella Bartolini · Tiziana Calamoneri ·
Emanuele Guido Fusco · Annalisa Massini ·
Simone Silvestri

© Springer Science+Business Media, LLC 2009

Abstract Mobile sensor networks are important for several strategic applications devoted to monitoring critical areas. In such hostile scenarios, sensors cannot be deployed manually and are either sent from a safe location or dropped from an aircraft. Mobile devices permit a dynamic deployment reconfiguration that improves the coverage in terms of completeness and uniformity. In this paper we propose a distributed algorithm for the autonomous deployment of mobile sensors called Push & Pull. According to our proposal, movement decisions are made by each sensor on the basis of locally available information and do not require any prior knowledge of the operating conditions or any manual tuning of key parameters. We formally prove that, when a sufficient number of sensors are available, our approach guarantees a complete and uniform coverage. Furthermore, we demonstrate that the algorithm execution always terminates preventing movement oscillations. Numerous simulations show that our

algorithm reaches a complete coverage within reasonable time with moderate energy consumption, even when the target area has irregular shapes. Performance comparisons between Push & Pull and one of the most acknowledged algorithms show how the former one can efficiently reach a more uniform and complete coverage under a wide range of working scenarios.

Keywords Coverage completeness · Coverage uniformity · Distributed algorithm · Mobile sensor networks · Self deployment

1 Introduction

Research in the field of mobile wireless sensor networks is motivated by the need to monitor hostile environments such as wild fires, disaster areas, toxic regions or battlefields, where static sensor deployment cannot be performed manually. In these working settings, sensors may be dropped from an aircraft or sent from a safe location. Mobile sensors can dynamically adjust their position to improve the coverage with respect to their initial deployment.

This paper addresses the problem of coordinating sensor movements to reach a more satisfactory deployment in terms of coverage extension and uniformity.

Centralized solutions to this problem are inefficient because they require either a prior assignment of sensors to positions, or a starting topology that ensures the connectivity of all sensors (for global coordination purposes). On the one hand, a prior assignment is inapplicable because it requires an excessive amount of movements to deploy sensors independently of their initial position. On the other hand, connectivity cannot be guaranteed in any starting

Animations and the complete code of the proposed algorithm are available for download at the address
http://www.dsi.uniroma1.it/~novella/mobile_sensors/.

N. Bartolini (✉) · T. Calamoneri · E. G. Fusco ·
A. Massini · S. Silvestri
Department of Computer Science,
“Sapienza” University of Rome, Rome, Italy
e-mail: bartolini@di.uniroma1.it

T. Calamoneri
e-mail: calamo@di.uniroma1.it

E. G. Fusco
e-mail: fusco@di.uniroma1.it

A. Massini
e-mail: massini@di.uniroma1.it

S. Silvestri
e-mail: simone.silvestri@di.uniroma1.it

scenario. Therefore, feasible and scalable solutions should employ a distributed scheme according to which sensors make local decisions to meet global objectives.

When designing solutions to the deployment problem, energy consumption is an important issue. Indeed, due to the limited power available, each sensor should coordinate with others with very few messages and should reach its position traversing small distances. Energy consumption should also be controlled by uniformly placing redundant sensors when available. In fact, a uniformly redundant coverage of the AoI allows to prolong the network lifetime, for example by allowing an alternative activation of sensors without any loss of coverage. A redundant sensor placement has also several benefits as it allows a better target sensing, stronger environmental monitoring, and fault tolerance capabilities.

The main contribution of this paper is an original fully distributed algorithm for mobile sensor deployment called Push & Pull, which is radically different from any previous one. Most of the existing approaches fall into one of two main categories, as they are either inspired by molecular physics [1–8] or by computational geometry [9–13]. In general, they aim at reaching a final deployment which is similar to the one targeted by our algorithm. Nevertheless, the solutions inspired by physical models usually tend to non-stable deployment, due to the dynamicity of the equilibrium that characterizes molecular systems. Hence such solutions necessitate proper countermeasures to ensure a gradual decrease of movements. On the other hand the approaches inspired by computational geometry are often unable to handle concave AoIs and lead to non-uniform deployments.

The design of our solution follows the grassroots approach [14] to autonomic computing. Self-organization emerges without the need of external coordination or human intervention as the sensors autonomously adapt their position on the basis of a local view of the surrounding scenario. This way our algorithm shows the basic self-* properties of autonomic computing, i.e. self-configuration, self-adaptation and self-healing.

This algorithm produces a hexagonal tiling by spreading sensors out of high density regions and attracting them towards coverage holes. Decisions regarding the behavior of each sensor are based on locally available information and do not require any prior knowledge of the operative scenario or any manual tuning of key parameters. Location awareness is only necessary in the case of sensor deployment over a specific target area, whereas this capability is not required when sensors are to be deployed in an open environment.

We formally prove that our algorithm terminates and provides a complete coverage regardless of the particular shape of the AoI; moreover, we propose a variant that exploits redundant sensors to produce a k -coverage, where

k depends on the number of the available sensors and on the shape and extension of the AoI.

We ran numerous simulations to evaluate the performance of our algorithm and compare it to existing solutions. Experimental results show that our algorithm reaches a complete and stable coverage within reasonable time with moderate energy consumption, even when the target area has an irregular shape. It turns out that our proposal provides better performance than one of the most acknowledged and cited algorithms [9]. Furthermore, our solution also outperforms previous approaches producing a redundant coverage with guaranteed uniformity.

This paper is organized as follows. In Sect. 2 we describe the Push & Pull algorithm. We devote Sect. 3 to a discussion on the implications of coverage uniformity on fault tolerance and network lifetime. In this section we also propose an algorithm variant which privileges uniformity over other performance requirements. In Sect. 4 we formally prove some important properties of the final deployment, namely termination, coverage completeness and uniformity. The simulation analysis is shown in Sect. 5. Section 6 describes the state of the art, while Sect. 7 concludes the paper.

2 The Push & Pull algorithm

In order to make the exposition clearer, we outline the algorithm, before giving deeper details.

2.1 The idea

Sensors aim at realizing a complete and uniform coverage of the AoI by means of a hexagonal tiling. Notice that the hexagonal tiling corresponds to a triangular lattice arrangement, that is the one that guarantees optimal coverage and density, as discussed in [15], and connectivity, as we detail in Sect. 4.3. The algorithm starts with the concurrent creation of several tiling portions. Every sensor not yet involved in the creation of a tiling portion gives start to its own portion in an instant which is randomly selected in a given time interval.

In the following, when we talk about s_{init} we refer, more in general, to any starter.

The algorithm mandates that four main activities are carried out in an interleaved manner. The combination of the described activities expands the tiling and, at the same time, does its best to uniformly distribute redundant sensors over the tiled area, preventing oscillations.

2.1.1 Snap activity

The sensor s_{init} elects its position as the center of the first hexagon of its tiling portion. It selects at most six sensors

among those located within its *transmission radius* R_{tx} and makes them snap to the center of adjacent hexagons. Such deployed sensors, in turn, give start to their own selection and snap activity, thus expanding the boundary of the current tiling portion. The sensors that are positioned in the center of a hexagon according to the snap activity, are hereafter referred to as *snapped sensors*. This activity continues until no other snaps are possible, because either the whole AoI is covered, or the boundary tiles do not contain any un-snapped sensors.

2.1.2 Push activity

After the completion of their snapping activity, snapped sensors may still be surrounded by non-snapped sensors located inside their hexagon, hereafter referred to as their *slaves*. In this case, they proactively push such slaves towards lower density areas located within their transmission range. Consequently, slaves being in overcrowded areas migrate to low density zones, thus accelerating the coverage process and enhancing its uniformity. A snapped sensor stops the push activity when the maximum detected density difference does not exceed one sensor.

2.1.3 Pull activity

Snapped sensors may detect a coverage hole adjacent to their hexagon and may not find available sensors to make them snap. In this case, they send hole trigger messages, and reactively attract non-snapped sensors and make them fill the hole. Such sensors keep on advertising the presence of a hole until either the holes is filled or a timeout occurs.

2.1.4 Tiling merge activity

The possibility that many sensors act as starters can give rise to several tiling portions with different orientations. In order to characterize and distinguish each tiling portion, the time-stamp of each starter is included in the header of all messages. As a result, messages coming from sensors located in different tiling portions will be characterized by different starter time-stamps. Our algorithm provides a mechanism to merge all these tiling portions into a unique regular and uniformly oriented tiling. When the boundaries of two tiling portions come in radio proximity with each other, the one with older starter time-stamp absorbs the other one by making its snapped sensors move into more appropriate snapping positions.

Figure 1 shows an example of the execution of the first two activities. Namely, Fig. 1(a) depicts the starting configuration, with nine randomly placed sensors and Fig. 1(b) highlights s_{init} starting the hexagonal tiling. In Fig. 1(c) the starter sensor s_{init} selects six sensors to make them snap in

adjacent hexagons, according to the minimum distance criterion. Figure 1(d) shows the configuration after the snap activity of s_{init} . In Fig. 1(e), a just deployed sensor starts a new snap activity while s_{init} starts the push activity sending a non-snapped sensor to a lower density hexagon. In Fig. 1(f) one of the deployed sensors causes the snap of the sensor just received from the starter, thus leading to the final configuration. Figure 2 shows an example of the execution of the tiling merge activity. In particular, Fig. 2(a) shows two tiling portions meeting each other. The portion on the left has the oldest time-stamp, hence it absorbs the other one. Two nodes of the right portion detect the presence of an older tiling and abandon their original position (Fig. 2b) to honor snap commands coming from a sensor of the left portion (Fig. 2c). These just snapped sensors, now belonging to the older portion, detect the presence of three nodes belonging to the right portion (Fig. 2d) and make them snap as soon as they leave their original tiling portion (Fig. 2e–f).

We defer the introduction of the example regarding the pull activity to the next section when more details will be available to clarify the explanation.

2.2 Details of Push & Pull

In order to describe the algorithm in more detail, we give some definitions and specify the operative setting.

Let V be a set of equally equipped sensors able to determine their own location, endowed with boolean sensing capabilities. We adopt an isotropic communication model and assume that sensors are in active mode for all the deployment phase. We set the hexagon side length l_h to the *sensing radius* R_s . This setting guarantees both coverage and connectivity when $R_{tx} \geq \sqrt{3}R_s$. This requirement is not restrictive as most wireless devices can adjust their transmission range by properly setting their transmission power.

All sensors that are neither snapped nor slaves are called *free*. Given a sensor x , snapped to the center of a hexagon, we denote by $S(x)$ the set of slaves of x and by $Hex(x)$ the hexagonal region whose center is covered by x . We define $L(x)$ the set composed by the sensors located in radio proximity from x (i.e. the free sensors in radio proximity from x the slaves $S(x)$). We also refer to $VP(x)$ (vacant positions) as to the set of positions detected by the sensor x at the center of the hexagons adjacent to $Hex(x)$ that are not yet occupied by any snapped sensor.

We now give additional details on the activities sketched in Sect. 2.1.

2.2.1 Snap activity

At the beginning of the deployment process, each sensor may act as starter of a snap activity from its initial location

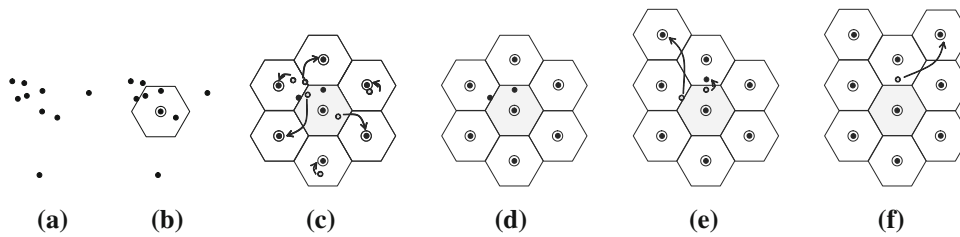


Fig. 1 An example of snap and push activities: **a** starting configuration; **b** s_{init} snaps itself at the center of the first tile; **c** s_{init} selects six sensors to make them snap in the adjacent hexagons; **d** configuration after the snap activity of s_{init} ; **e** s_{init} pushes a sensor to a nearby

hexagon, while a just deployed sensor gives rise to a new snap activity; **f** a snapped sensor causes the snap of the sensor that it has just received from the starter

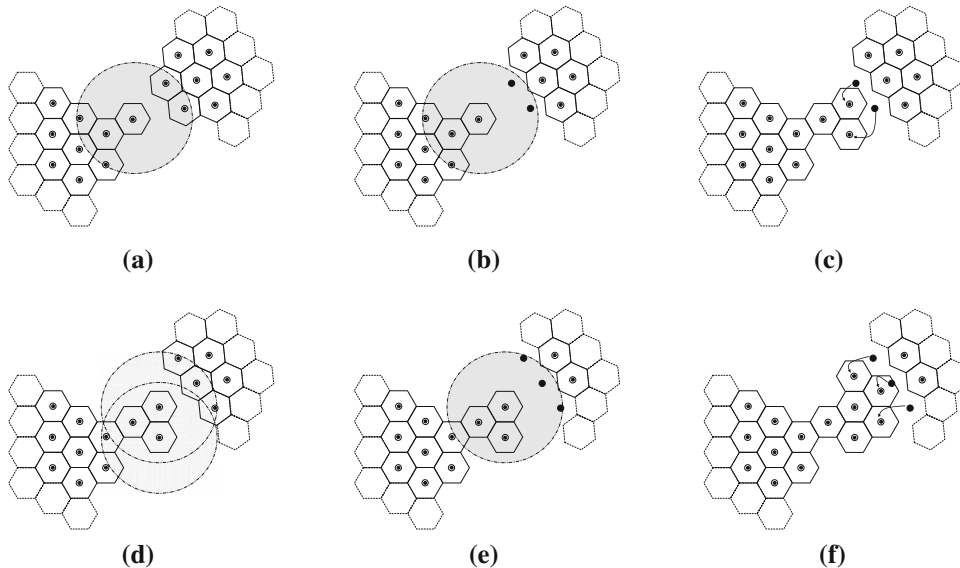


Fig. 2 An example of tiling merge activity: **a** two tiling portions meet each other (the one on the left has the oldest time-stamp); **b** two nodes of the right portion detect the presence of the older portion; **c** the two nodes abandon their original portion and are snapped to new

positions in the older portion; **d** these just snapped sensors detect the presence of three nodes belonging to the right portion and **e** and **f** make them snap

at an instant randomly chosen over a given time interval. In order to propagate a tiling portion, a snapped sensor x performs a *neighbor discovery*, that allows x to gather information regarding $S(x)$ and all the free and snapped sensors located in radio proximity from x and the positions belonging to $VP(x)$. To give start to new snap activities, x selects the sensor in $L(x)$ which is the closest to each uncovered position and snap it there. A snapped sensor leads the snapping of as many adjacent hexagons as possible and gives start to the push activity, as described in Fig. 3.

If some of the positions in $VP(x)$ cannot be covered because $L(x)$ does not contain enough sensors, x starts the pull activity. If otherwise all the hexagons adjacent to $Hex(x)$ have been covered and $VP(x) = \emptyset$, x stops any further snapping, and uses the available slaves (if any) to give start to the push activity.

Figure 4 shows a detailed flow chart of the Snap, Push and Pull activities, in agreement with the underlying coordination protocol which is described in [16]. In this

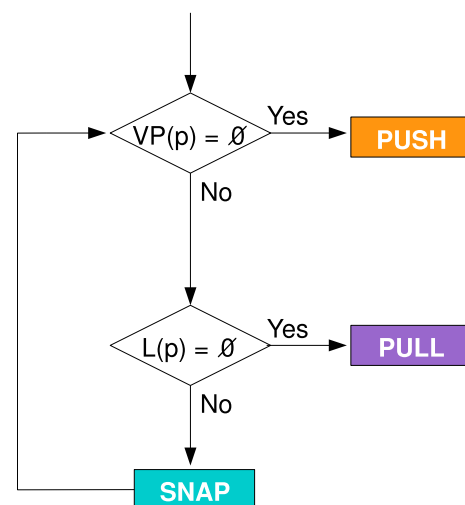


Fig. 3 Behavior of the snapped sensor p

figure, for clarity, we denote with $G(x)$ the set of snapped sensors located in hexagons adjacent to $Hex(x)$.

2.2.2 Push activity

Given two snapped sensors x and y located in radio proximity to each other, x may offer one of its slaves to y and push it inside its hexagon if $|S(x)| \geq |S(y)| + 1$. Note that, if $|S(x)| = |S(y)| + 1$, the flow of a sensor from $Hex(x)$ to $Hex(y)$ leads to a symmetric situation in which $|S(y)| = |S(x)| + 1$ possibly causing endless cycles. In such cases we restrict the push activity to only one direction: x pushes its slave to y only if $id(y) < id(x)$, where $id(\cdot)$ is a function initially set to the unique identity code of the sensor radio device (notice that this is not the only possibility, $id(\cdot)$ could be set for example to a random non negative value). We formalize these observations by defining the following *Moving Condition*, that enables the movement of a sensor from $Hex(x)$ to $Hex(y)$:

$$|S(x)| > |S(y)| + 1 \vee \{|S(x)| = |S(y)| + 1 \wedge id(x) > id(y)\}$$

The snapped sensor x executes a push action by sending one of its slaves s towards the hexagon of a snapped sensor y .

The destination hexagon $Hex(y)$ is selected such that x verifies the moving condition with respect to y . In particular, as destination of the push action, x selects the closest hexagon among those with the lowest number of slaves. Among the sensors which can be pushed to the destination, x selects the closest to $Hex(y)$.

If a snapped sensor receives a neighbor discovery request while involved in a push activity, it replies as if the ongoing movements were already concluded. Indeed, if a snapped sensor communicated its own number of slaves without keeping into account the ongoing movements, it could cause inconsistencies (for example either too many sensors could move to the same hexagon or the same sensor could be offered to several snapped sensors). The snapped sensors involved in a push activity always alert their neighborhood of the changed number of slaves.

2.2.3 Pull activity

The sole snap and push activities are not sufficient to ensure the maximum expansion of the tiling. This may happen when there exists a direction in which the density decreases of at most one sensor at a time, and the Moving Condition is false due to the order relationship induced by function $id(\cdot)$. The same problem may cause also non-uniform coverage. For this reason, we introduce the pull activity that makes use of a *trigger mechanism* when some holes occur. Namely, let x be a snapped node detecting a hole in an adjacent hexagon, with $S(x) = \emptyset$. If x has not the possibility to receive any slave from its neighbor hexagons, i.e. the Moving Condition is not verified for any of them, then it activates the following trigger mechanism. Sensor x temporarily alters the value of its id function to 0 and notifies its neighbors of this change by means of a *trigger notification message*. This could be sufficient to

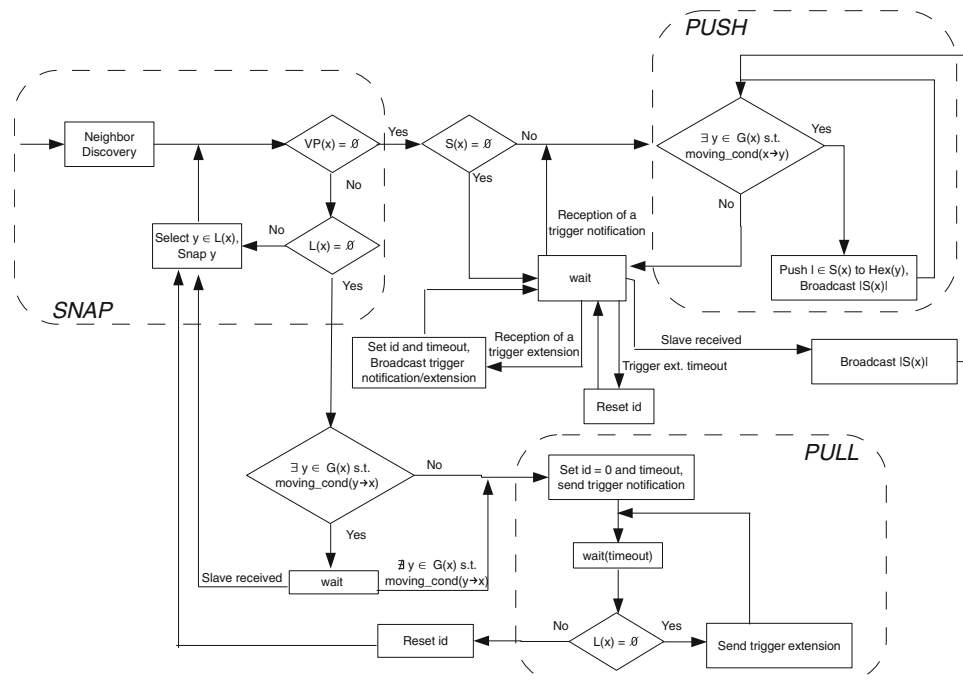


Fig. 4 A detailed flow chart of the Snap, Push and Pull activities

make the Moving Condition true with at least a snapped neighbor, so x waits until either a new slave comes into its hexagon or a timeout occurs. If a new slave enters $Hex(x)$, x sets back its id value and snaps the new sensor, thus filling the hole. If the timeout expires and the hole has not been covered yet, x extends the trigger to its adjacent hexagons by sending them a *trigger extension message*. As a consequence, the snapped neighbors of x set their id value to 1 and send the related trigger notification message. This mechanism is iterated by x over snapped sensors at larger and larger distance in the tiling until the hole is covered. Each snapped sensor involved in the trigger extension mechanism sets its id to a value that is proportional to the distance from x . All the timeouts related to each new extension are set proportionally to the maximum distance reached by the trigger mechanism. At this point, as a consequence of timeouts, each involved node sets back its id to the original value. In order to better detail the trigger mechanism, we show the following example. Figure 5(a) shows a tiled AoI with a coverage hole in the bottom left corner. Snapped nodes detecting the hole set their id to 0 and send a trigger notification message. As their neighbors do not have slaves, they need to send a trigger extension message, provoking a propagation of the id modification (see Fig. 5b). As soon as the unique snapped sensor with a slave alters its id to honor the trigger mechanism, the Moving Condition is satisfied and therefore the slave is pushed towards a snapped sensor that is closer to the hole, as shown in Fig. 5(c). In Fig. 5(d) the hole coverage is highlighted and, after the timeouts expire, all ids are set back to the previous values (Fig. 5e).

It should be noted that more snapped nodes adjacent to the same hole may independently activate the trigger mechanism, possibly at different times. In this case, if a node receives a trigger extension message from two or more nodes, it honors only the one with the lowest id . The detection of several holes may cause the same node y to receive several trigger extension messages. These are stored in a pre-emptive priority queue, privileging the messages related to the closest hole.

2.2.4 Tiling merge activity

If several sensors act as starters, several tiling portions can be generated with different orientations. By contrast, our algorithm aims to cover the AoI with a perfectly regular tiling thus minimizing overlaps of the sensing disks and enabling a complete and uniform coverage. Hence, we design a merge mechanism according to which as soon as a sensor x receives a neighbor discovery message from another tiling portion it joins the oldest one (it discriminates this situation by evaluating the time-stamp of the starter action). It should be noted that the detection of the

sole neighbor discovery messages is sufficient to ignite the tiling merge activity because such messages are sent after any tiling expansion and, if two tiling portions come in radio proximity, at least one of them is increasing its extension. In the following, we call G_{old} and G_{new} the tiling portions with lower and higher time-stamp, respectively.

We distinguish three possible cases:

- 1) x belongs to G_{new} : if x is a slave, sensor x switches its state to free and communicates its new state to the neighborhood. From now on x will honor only the messages coming from G_{old} and will ignore those from G_{new} . This proactive communication is needed to advertise the presence of G_{new} when there is no message exchange within G_{new} perceivable by the sensors in G_{old} . This way, the snapped sensor to which x belonged, can properly update its slave set. If x is instead a snapped sensor, it cannot immediately switch its state to free because of its leading role inside G_{new} (e.g. it leads the slave sensors in $S(x)$ and performs push and pull activities). Hence, x temporarily assumes a hybrid role: it declares itself as free to the nodes of G_{old} and, at the same time, acts as a snapped sensor in G_{new} until it receives a snap command coming from G_{old} . After the reception of such a snap command, x moves to the new snap position and elects one of its slave as a substitute. If no slave is available, x advertises its departure to its neighbors in G_{new} .
- 2) x belongs to G_{old} : if x is a slave, it ignores all messages from G_{new} . If x is snapped, it performs a neighbor discovery, ignores all messages coming from G_{new} (apart from the neighbor discovery replies) and honors only messages from G_{old} . Observe that the neighbor discovery is necessary to ignite the merge mechanism. The neighbor discovery allows each snapped sensor in G_{old} to collect complete information about nearby sensors that previously belonged to G_{new} .
- 3) x is free: the sensor x honors only messages from G_{old} and ignores those from G_{new} .

2.3 Balancing energy consumption

According to the previous description of Push & Pull, slaves consume more energy than snapped sensors, because they are involved in a larger number of message exchanges and movements. We introduce a *mechanism to balance the energy consumption* over the set of available sensors making them exchange their roles. This mechanism is similar to the technique of *cascaded movements* introduced in [13]. Namely, any time a slave has to make a movement across a hexagon as a consequence of either push or pull activities, it evaluates the opportunity to substitute itself with the snapped sensor of the hexagon it is traversing. The

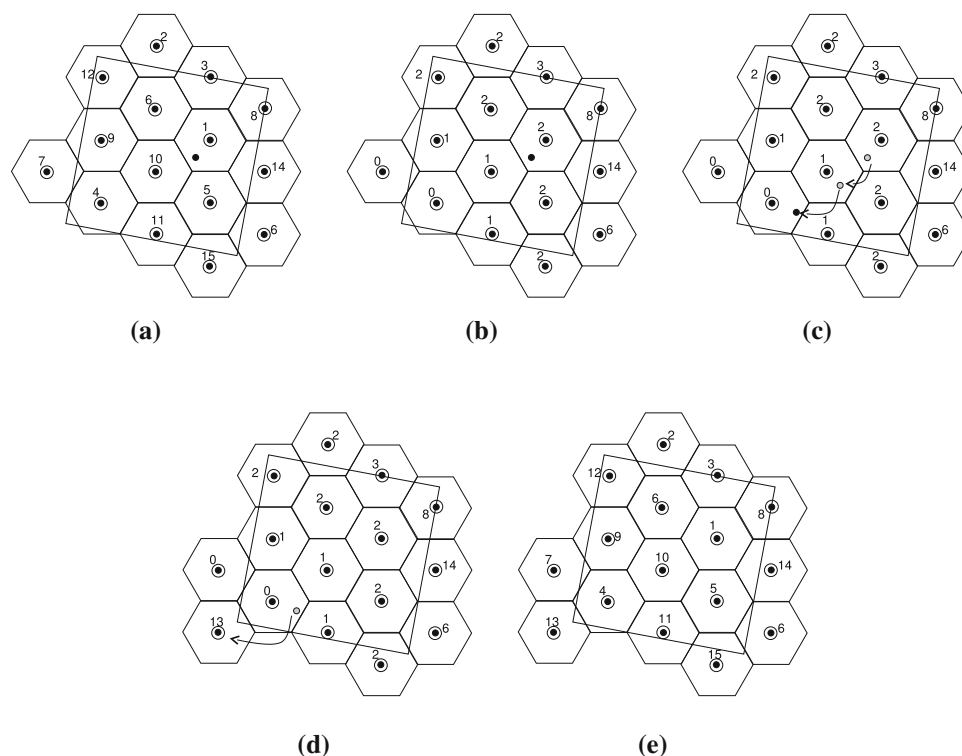


Fig. 5 An example of the pull activity: **a** a tiled AoI with a coverage hole in the bottom left corner; **b** the two snapped nodes detecting the hole set their *id* to 0 and send a trigger notification message that is

propagated by their neighbors which modify their *id*; **c** the closest available slave moves towards the hole; **d** the hole is covered and **e** all *ids* are set back to the previous values

criterion at the basis of this mechanism is that two sensors exchange their role whenever the energy imbalance is reduced. As a result, the energy balance is significantly enhanced, though the role exchange has a small cost for both the slave and the snapped sensor involved in the substitution. Indeed, the slave sensor has to reach the center of the current hexagon and perform a *profile packet* exchange with the snapped sensor that has to move towards the destination of the slave. A profile packet contains the key information needed by a sensor to perform its new role after a substitution.

2.4 The sensor coordination protocol

The implementation of our algorithm requires the definition of a protocol for the coordination of activities among locally communicating sensors. The coordination protocol provides the rules to solve contentions that may happen in several cases. For example, two or more snapped sensors can decide to issue a snap command to more than one sensor towards the same hexagon tile or a low density hexagon can be selected by several snapped sensors as candidate for receiving redundant slaves. These contentions are solved by properly scheduling actions according to message time-stamps and by advertising related decisions as soon as they are made.

This protocol is designed to minimize energy consumption in terms of message exchanges, which is possible because the algorithm decisions are only based on a small amount of local information. Furthermore, we assume that the protocol of Push & Pull is implemented over a communication protocol stack which handles possible errors and losses that may occur on the radio channels by means of timeout and retransmission mechanisms. We do not give any further detail on the protocol underlying Push & Pull as it is beyond the scope of this paper. The interested reader can refer to [16].

3 A discussion on uniformity implications

The execution of Push & Pull guarantees coverage uniformity only if the number of available sensors is exactly the minimum for the given orientation of the final grid. If redundant sensors are available, their movements are regulated by the moving condition, that precludes the flow of redundant sensors from high density to low density hexagons if the difference between the local densities is only of one sensor. This may cause local formation of a stairwise density distribution when the order function is monotonically increasing in the precluded flow direction. An example of such situations is depicted in Fig. 6, where for

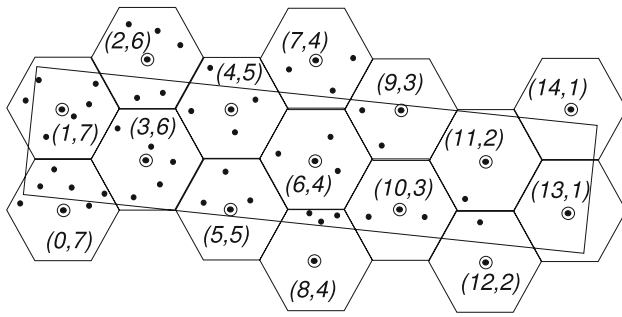


Fig. 6 Local formation of a stairwise density distribution

each hexagon the elements of the pairs represent the order value and the number of sensors, respectively.

The length of these formations is usually very short due to the random distribution of the order value over the set of sensors. The worst case, albeit improbable, happens when a stairwise distribution is as long as the diameter of the AoI.

In order to guarantee the uniformity of the sensor deployment even in the presence of redundant sensors, we introduce a *shrunked grid mode* as a variant of the Push & Pull algorithm. From now on, we will refer to the basic version with the name PP1 and to the shrunked grid mode with the name PP2. In Sect. 4 we prove that PP2 enables a uniformly redundant coverage, and we provide metrics and related formulas to calculate the guaranteed redundancy level.

In order to formally describe such mode we introduce the following definition: the *tight number of sensors* is the maximum number of hexagons of side length l_h necessary to cover the AoI for each possible initial position of the sensor set and each possible tiling orientation. This number represents the maximum number of sensors that can be necessary to cover the AoI with a hexagonal tiling of side l_h , regardless of the position and orientation of the grid.

We denote this number by $N_{\text{tight}}(l_h, \text{AoI})$, for short $N_{\text{tight}}(l_h)$, as the AoI is clear from the context. An upper bound on this number can be calculated by increasing the AoI with a border whose width is the maximal diameter of the tiling hexagon that is $2l_h$ and dividing the area of such a region (call it $\text{AoI}'(l_h)$) by the hexagon area. Formally

$$N_{\text{tight}}(l_h) \leq \left\lceil \frac{\text{Area}(\text{AoI}'(l_h))}{(3\sqrt{3}/2)l_h^2} \right\rceil \quad (1)$$

It should be noted that this upper bound is valid in the general case but its calculation can be improved if the AoI has a particularly regular shape.

PP2 is executed with a shorter hexagon side length. Namely, l_h is set to reduce as much as possible the number of slave sensors in the whole deployment, and is calculated as the value that makes the number of sensors equal to the tight number for that side length, and therefore is the inverse function of $N_{\text{tight}}(\cdot)$, calculated in N , where N is the number of sensors. More formally, $l_h = N_{\text{tight}}^{-1}(N)$. Since

function $N_{\text{tight}}(\cdot)$ is not known, we calculate an upper bound on l_h as the inverse of the upper bound on $N_{\text{tight}}(l_h)$, because $N_{\text{tight}}(\cdot)$ is a decreasing function of l_h .

PP1 and PP2 produce sensor deployments with different performance in terms of energy consumption and fault tolerance. The choice between them depends on the particular application requirements, as discussed below here.

In terms of energy consumption, PP2 performs worse than PP1, as we will show and motivate in Sect. 5. Nevertheless, as it guarantees a uniformly redundant coverage, it makes possible the use of topology control algorithms [17] that permit selective sensor activation saving energy during the operative phase, which, in turn, follows the deployment phase of the network. Moreover, this mode is beneficial when the application requires enhanced environmental monitoring and strong fault-tolerance capabilities. From the fault tolerance point of view, PP1 may be endowed with a periodic polling scheme to detect new possible coverage holes determined by sensor failures. This way, the detection of new holes causes the restart of the algorithm and the execution of the pull activity that attracts redundant sensors possibly located far from the coverage hole. Hence, PP1 presents self-healing properties which are not found in previous solutions. An example of such a mechanism is shown in Fig. 7. Figure 7(a) shows the deployment achieved after the application of PP1. Figure 7(b) shows a subsequent situation in which a certain number of sensors failed, creating a coverage hole. The presence of such a coverage hole is detected by the nearby sensors, which give start to the pull activity, attracting some redundant sensors located in higher density areas. Figure 7(c) shows an intermediate situation, before the redundant sensors succeed in covering the hole, as shown in Fig. 7(d).

Instead, PP2 can tolerate several failures, even closely located, in a number which is proportional to the redundancy level. By contrast, PP2 is not able to fill newly detected holes, because (almost) all sensors are snapped and do not take part in the movements determined by the pull activity. For this reason we do not introduce any polling mechanism in PP2, as there are too few slaves available and it would produce an inefficient pull activity in the case of a hole detection. On the other hand such version guarantees a uniform redundant coverage, if a sufficient number of sensors are available, tolerating even numerous sensor failures, as shown in Fig. 8, which depicts the occurrence of several co-located sensor failures without any loss of coverage.

4 Algorithm properties

In this section we prove some key properties of the Push & Pull algorithm: coverage, connectivity and termination.

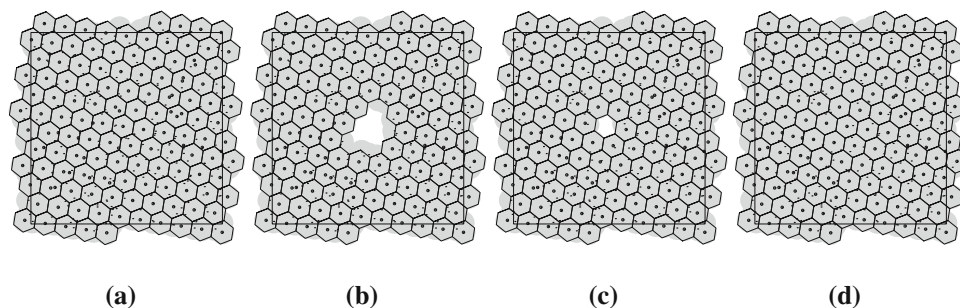


Fig. 7 Self-healing capability of PP1: **a** sensor deployment after the execution of PP1; **b** failure of several closely located sensors; **c** an intermediate step in the execution of the pull activity; **d** the coverage hole is filled

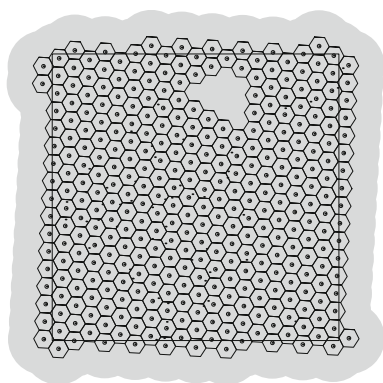


Fig. 8 Fault tolerance of PP2 to the failure of several closely located sensors

4.1 Coverage completeness

In this subsection we prove that Push & Pull (both modes) guarantees the complete coverage.

Theorem 1 *Algorithm Push & Pull guarantees the complete coverage, provided that at least the tight number of sensors $N_{\text{tight}}(l_h)$ are available.*

Proof Let us assume that a coverage hole exists. As our algorithm is designed, this hole will eventually be detected by a sensor x . Furthermore, by the hypothesis on the number of sensors, it certainly exists a hexagon with at least one redundant slave. Let us call C_x the connected component containing sensor x . Two different cases may occur depending on the position of the redundant slaves with respect to C_x .

- (1) A redundant slave exists in C_x : the snapped sensor x starts the trigger mechanism that eventually reaches a redundant slave so that it is pushed towards x and consequently it fills the hole.
- (2) All redundant slaves are located in connected components different from C_x : the area surrounding each connected component is in fact a coverage hole that will eventually be detected by a snapped node located at the boundary. According to what stated for the case

1), all the separated connected components containing redundant slaves will expand themselves to fill as many coverage holes as possible. Since, by hypothesis, the number of sensors is at least $N_{\text{tight}}(l_h)$, it certainly exists a component containing redundant slaves that will eventually merge in C_x , leading to the situation described in the case 1), thus proving the theorem. \square

Notice that, having $N_{\text{tight}}(l_h)$ sensors is a sufficient condition to guarantee the coverage completeness, but this number is not also necessary. Indeed, $N_{\text{tight}}(l_h)$ is calculated as the maximum among all the minimum numbers of sensors necessary to cover the AoI, for each orientation of the final grid with side length l_h . So it is possible that $N_{\text{tight}}(l_h)$ is larger than the number of sensor strictly necessary for a fixed orientation and position of the oldest starter.

4.2 Coverage uniformity

We consider two different coverage redundancy metrics. The first metric evaluates the coverage only in correspondence to the hexagonal grid points. This metric, named *grid coverage level*, is of interest for the applications that do not require a continuous sensing of the area of interest but rely on interpolation of local measurements. On the contrary, the second metric, named *continuous coverage level*, is more restrictive and is introduced to evaluate the coverage redundancy at each point of the area of interest.

Definition 1 The *grid coverage level* is the minimum number of sensors covering each point of a regular grid.

Definition 2 The *continuous coverage level* is the minimum number of sensors covering any point of the area of interest.

In order to compute such metrics for PP1 and PP2, we introduce the following lemma. The values of continuous coverage levels are shown in Fig. 9, for an example scenario.

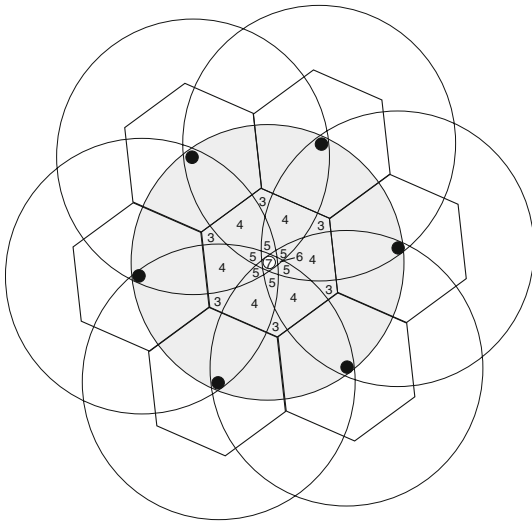


Fig. 9 An example of continuous coverage levels

Lemma 1 Given a triangular lattice of side l_h , any circle of radius R and centered in a point of the lattice contains

$$n(R) = \sum_{i=-\lfloor \frac{R}{\sqrt{3}l_h} \rfloor}^{\lfloor \frac{R}{\sqrt{3}l_h} \rfloor} \left(1 + 2 \left\lfloor \frac{\sqrt{R^2 - 3l_h^2 i^2}}{3l_h} \right\rfloor \right) + 4 \sum_{i=0}^{\lfloor \frac{R}{\sqrt{3}l_h} - \frac{1}{2} \rfloor} \left(1 + \left\lfloor \frac{\sqrt{R^2 - 3l_h^2 (i + \frac{1}{2})^2}}{3l_h} - \frac{1}{2} \right\rfloor \right)$$

points of the lattice.

Proof We observe that the points inside the circle of radius R and centered in any point of the lattice always lie in the same position with respect to the center of the circle (see Fig. 10), then we can slightly modify the reasoning for the well known Gauss' circle problem, dealing with squared grids.

Let the center of the circle be the origin of a Cartesian plane with axis aligned with the grid.

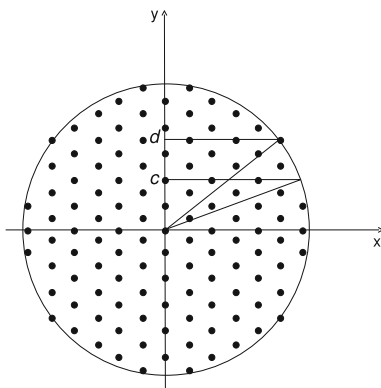


Fig. 10 Calculus of the grid coverage level

We count the points inside the circle considering them as arranged by horizontal rows.

The number of points in interval $(0, R]$ of the x axis is $\lfloor \frac{R}{3l_h} \rfloor$ and similarly in interval $[-R, 0)$. So, counting the origin, there are $1 + 2 \lfloor \frac{R}{3l_h} \rfloor$ points in interval $[-R, R]$.

Now we count the number of sensors lying on the rows having a sensor on the y axis.

Let us consider one of these rows lying on the line $y = c$, it contains $1 + 2 \lfloor \frac{\sqrt{R^2 - c^2}}{3l_h} \rfloor$ points. As two such consecutive rows in the same semiplane are $\sqrt{3}l_h$ far from each other, it follows that the whole number of sensors on all the rows having a sensor on the y axis and lying on the positive semiplane is

$$\sum_{i=1}^{\lfloor \frac{R}{\sqrt{3}l_h} \rfloor} \left(1 + 2 \left\lfloor \frac{\sqrt{R^2 - 3l_h^2 i^2}}{3l_h} \right\rfloor \right).$$

Finally, we count the number of sensor lying on the rows not having a sensor on the y axis.

Let us consider one such row lying on the line $y = d$; the sensor closest to the y axis has x -coordinate $\frac{3}{2}l_h$, so we consider the interval $\sqrt{R^2 - d^2} - \frac{3}{2}l_h$ long. Hence, the number of sensors on this row is $2 \left(1 + \left\lfloor \frac{\sqrt{R^2 - d^2} - \frac{3}{2}l_h}{3l_h} \right\rfloor \right)$. With arguments similar to the previous case, we have that the number of sensors lying on these rows in the positive semiplane is:

$$\sum_{i=0}^{\lfloor \frac{R}{\sqrt{3}l_h} - \frac{1}{2} \rfloor} 2 \left(1 + \left\lfloor \frac{\sqrt{R^2 - 3l_h^2 (i + \frac{1}{2})^2} - \frac{3}{2}l_h}{3l_h} \right\rfloor \right).$$

The result follows by summing all the described contributions. \square

Theorem 2 Under the assumption that at least a tight number of sensors are available, and the shrunk grid mode is enabled, algorithm Push & Pull guarantees a k grid coverage level, where $k = n(R_s)$.

Proof The definition of l_h and lemma 1 imply that, under the given assumptions, algorithm Push & Pull provides a complete coverage. Given the geometric regularity of the obtained deployment, every sensing circle surrounding a snapped sensor contains at least a fixed number k of snapped sensors belonging to the triangular lattice determined by the hexagonal grid deployment. As all sensors have the same sensing radius, the sensing redundancy level at the center of the circle is at least k .

In order to estimate the continuous coverage level of any sensor deployment, in [18] the authors introduce the notion of perimeter coverage. They define a sensor s to be k -

perimeter covered if all points in the perimeter of the sensing circle of s are covered by at least k sensors (not counting s).

The same authors also prove (see Theorem 1 in [18]) that the sensor deployment provides a continuous coverage level k if and only if each sensor is k -perimeter covered. \square

Theorem 3 *Under the assumption that at least a tight number of sensors is available, and the shrunk grid mode is enabled, algorithm Push & Pull guarantees a k continuous coverage level, where $k \geq \frac{n(R_s)-1}{3} + \frac{n(\sqrt{3}R_s)-n(R_s)}{6}$*

Proof According to the above cited theorem [18], the level of continuous coverage enabled by the algorithm Push & Pull can be calculated as the minimum perimeter coverage over all the snapped sensors. In order to calculate such coverage level, we distinguish two main contributions, the first one coming from sensors located inside the sensing circle of s , and the second one, coming from the sensors located outside.

All sensors located inside the sensing circle of s contribute to the perimeter coverage with a circular sector of amplitude α , with $\frac{2}{3}\pi \leq \alpha < \pi$. Since any of these sensors is symmetric to other five sensors inside the circle, with a rotation of $\pi/3$ centered in the position of sensor s , all the six of them contribute to at least a double coverage of the sensing circle perimeter of s . The sensors forming this first contribution amount to $n(R_s) - 1$ (not counting the sensor s itself), and all of them globally guarantee $2\lfloor \frac{n(R_s)-1}{6} \rfloor$ -perimeter coverage.

The second contribution is related to the sensors located outside the sensing circle of s . We note that the sensing circle of the sensors located farther than $2R_s$ from s do not intersect the sensing circle of s , while the sensing circle of sensors located at a distance d such that $\sqrt{3}R_s < d \leq 2R_s$ intersect the sensing circle of s , determining a circular arc of amplitude less than $\pi/3$. Since we are calculating a lower bound on the minimum perimeter coverage, we do not consider the contribution of this latter sensors as it does not guarantee a complete perimeter coverage and therefore may not affect its minimum value.

For this reason, as a second contribution to the perimeter coverage, we only consider the sensors located inside the circular crown determined by the radii R_s and $\sqrt{3}R_s$. This sensors contribute to the perimeter coverage with a circular sector of amplitude β , with $\pi/3 \leq \beta < \frac{2}{3}\pi$. Since any of these sensors is symmetric to other five sensors inside the crown, with a rotation of $\pi/3$ centered in the position of sensor s , all the six of them contribute to at least one single coverage of the sensing circle perimeter of s . The sensors forming this second contribution amount to $n(\sqrt{3}R_s) - n(R_s)$ and all of them globally guarantee a $\lfloor \frac{n(\sqrt{3}R_s)-n(R_s)}{6} \rfloor$ -perimeter coverage. Notice that the particular 3-axis symmetry, induced by the hexagonal tiling, makes it

possible to remove the floor operator from the two terms, as $n(R)-1$ is always divisible by 6.

By summing the two contribution to the perimeter coverage, we derive the claimed lower bound. \square

4.3 Coverage and connectivity

In this subsection we motivate the choice of the hexagonal tiling and the assumption that the sensors operate with $R_{tx} \geq \sqrt{3}R_s$, that is a less restrictive condition than usually required in the literature.

In [19], the authors demonstrate that coverage implies connectivity if and only if R_{tx} is twice the value of R_s . This statement is generally valid regardless of the particular distribution of the sensors over the AoI, be it a regular geometrical mesh or a random deployment. A hexagonal tiling with side length R_s is the one that minimizes node density while ensuring coverage completeness at the same time, as argued in [15]. Since our algorithm works exactly with this kind of tiling, which corresponds to a triangular lattice, we can relax the relationship between R_{tx} and R_s . If the sensors are regularly deployed on a hexagonal tiling, the distance between any two tiling neighbors is exactly $\sqrt{3}R_s$, implying the following result.

Theorem 4 *Under a complete triangular lattice coverage with side length R_s , a necessary and sufficient condition to guarantee connectivity is that $R_{tx} \geq \sqrt{3}R_s$*

4.4 Termination of Push & Pull

We conclude this section by proving the termination of our algorithm.

Let $L = \{\ell_1, \ell_2, \dots, \ell_{|L|}\}$ be the set of snapped sensors.

Definition 3 A *network state* is a vector \mathbf{s} whose i -th component represents the number of sensors deployed inside the hexagon $Hex(i)$ governed by the snapped sensor i . Therefore $\mathbf{s} = \langle s_1, s_2, \dots, s_{|L|} \rangle$ where $s_i = |S(i)| + 1$, $\forall i = 1, \dots, |L|$.

Definition 4 A state $\mathbf{s} = \langle s_1, \dots, s_{|L|} \rangle$ is *stable*, if the Moving Condition is false for each couple of snapped sensors in L located in radio proximity to each other.

Theorem 5 *Algorithm Push & Pull terminates in a finite time.*

Proof As long as new sensors are being snapped, the covered area keeps on growing. This process eventually ends either because the AoI has been completely covered or because the sensors have reached a configuration that does not allow any further expansion of the tiling. Due to Theorem 1 the latter can only happen when all sensors are snapped and thus the state of the network is stable. In order

to prove the theorem, it suffices to prove that, once the AoI is fully covered, the algorithm reaches a stable configuration in a finite time. Therefore we can consider the set of snapped sensors L as fixed. The value of the order function related to each snapped sensor, $id(\ell_i)$, is set during the unfolding of the algorithm, it can be modified only temporarily by the pull activity a finite number of times and remains steady onward. Let us define $f: \mathbb{N}^{|L|} \rightarrow \mathbb{N}^2$ as follows: $f(\mathbf{s}) = \left(\sum_{i=1}^{|L|} s_i^2, \sum_{i=1}^{|L|} s_i \cdot id(\ell_i) \right)$. We say that $f(\mathbf{s}) \succ f(\mathbf{s}')$ if $f(\mathbf{s})$ and $f(\mathbf{s}')$ are in lexicographic order. Observe that function f is lower bounded by the pair $(|L|, \sum_{i=1}^{|L|} id(\ell_i))$, in fact $1 \leq s_i \leq |V|$. Therefore, if we prove that the value of f decreases at every state change, we also prove that no infinite sequence of state changes is possible. To this purpose, let us show that every state change from \mathbf{s} to \mathbf{s}' causes $f(\mathbf{s}) \succ f(\mathbf{s}')$. Let us consider a generic state change which involves the snapped sensors x and y , with x sending a slave sensor to $Hex(y)$. We have that $s_i = s'_i \forall i \neq x, y$, and $s'_x = s_x - 1$ and $s'_y = s_y + 1$. As the transfer of the slave has been done according to the Moving Condition, two cases are possible: either $s_x > s_y + 1$, or $(s_x = s_y + 1) \wedge (id(x) > id(y))$. In the first case, the inequality $s_x > s_y + 1$ implies that $\sum_{i=1}^{|L|} s_i^2 > \sum_{i=1}^{|L|} s_i'^2$. In the second case, since $s_x = s_y + 1$ and $id(x) > id(y)$, lead to $\sum_{i=1}^{|L|} s_i^2 = \sum_{i=1}^{|L|} s_i'^2$ and $\sum_{i=1}^{|L|} s_i \cdot id(\ell_i) > \sum_{i=1}^{|L|} s_i' \cdot id(\ell_i)$. Therefore in both cases $f(\mathbf{s}) \succ f(\mathbf{s}')$. The function f is lower bounded and always decreasing by discrete quantities (integer values) at any state change. Thus, after a finite number of steps, it is impossible to perform a further state change, i.e. the network will be in a *stable state* in a finite time. \square

5 Simulation results

In order to evaluate the performance of Push & Pull and to compare it with previous solutions, we developed a

simulator using the wireless module of the OPNET modeler software [20].

We compare our proposal to one of the most acknowledged and cited algorithms [9], which is based on the construction of the Voronoi diagram determined by the current sensor deployment. According to this approach, each sensor adjusts its position on the basis of a local calculation of its Voronoi cell. This information is used to detect coverage holes and, consequently, calculate new target locations according to three possible variants. Among these variants we chose Minimax, that gives better guarantees in terms of coverage extension. Of this algorithm we adopted all the mechanisms provided to preserve connectivity, to guarantee the algorithm termination, to avoid oscillations and to deal with position clustering [9]. In the rest of this section this algorithm will be named VOR_{MM} .

We set the parameters $R_{tx} = 11$ m and $R_s = 5$ m. Such values satisfy the VOR_{MM} requirement $R_{tx} > 2 R_s$ detailed in [9] and do not significantly affect the qualitative evaluation of Push & Pull. The sensor speed is set to 1 m/s.

5.1 Examples of mobile sensor deployment

We show some examples of deployment evolution under the two Push & Pull modes: PP1 and PP2.

Figures 11 and 12 give a synthetic representation of how the sensor deployment evolves under PP1 and PP2, respectively, when 400 sensors are initially located in a high density region. The AoI has a complex shape in which a narrow connects two square regions $40 \text{ m} \times 40 \text{ m}$. Notice that previous approaches fail when applied to such irregular AoIs. For example, VOR_{MM} does not contemplate the presence of concavity in the AoI, while the virtual force based approaches are not able to push sensors through narrow [1].

As a second example of sensor deployment, we show experiments conducted with three different starting

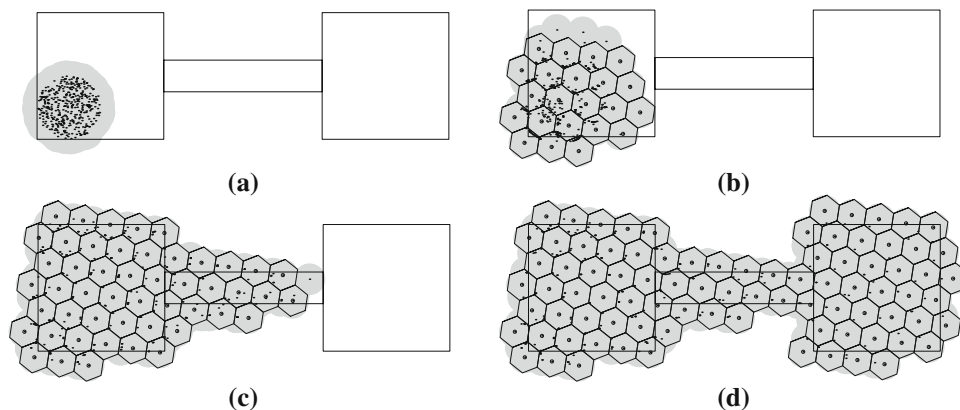


Fig. 11 Coverage of an irregular AoI under PP1

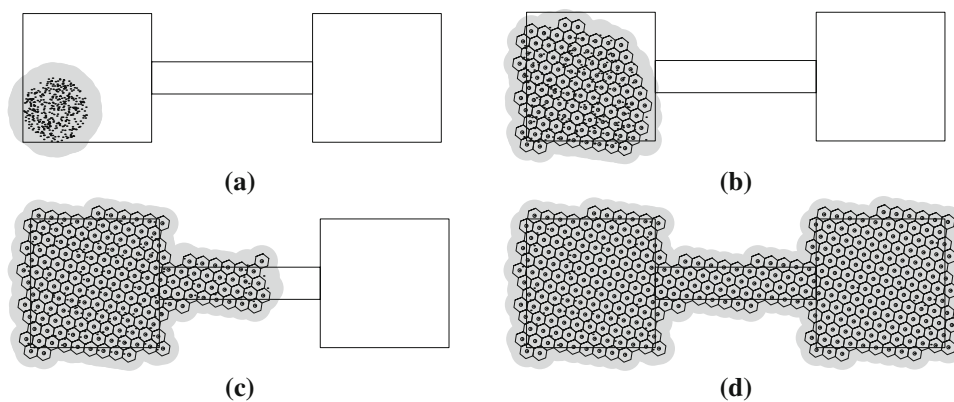


Fig. 12 Coverage of an irregular AoI under PP2

configurations over an AoI which is a square $80\text{ m} \times 80\text{ m}$. More precisely, in the first configuration, the initial deployment evidences a trail of sensors which crosses the AoI, as shown in Fig. 13(a). In the second configuration the sensors are densely placed in a corner of the AoI, as shown in Fig. 14(a). In the third configuration the initial deployment consists in a high density region at the center of the AoI, as shown in Fig. 15(a).

Notice that the first two initial deployments reflect the realistic scenarios in which sensors are dropped from an aircraft and sent from a safe location at the boundaries of the AoI. The third deployment is introduced as is widely studied in the literature, see for example [9, 10].

In Figs. 13, 14 and 15, the subfigures indicated with (b), (c) and (d) show the final deployments achieved by PP1, PP2 and VOR_{MM} respectively.

5.2 Performance comparisons

In the following we compare the performance of PP1, PP2 and VOR_{MM} when executed over a squared AoI, $80\text{ m} \times 80\text{ m}$.

In order to make reliable performance comparisons, we show the average results of 30 simulation runs (conducted by varying the seed for the generation of the initial deployment).

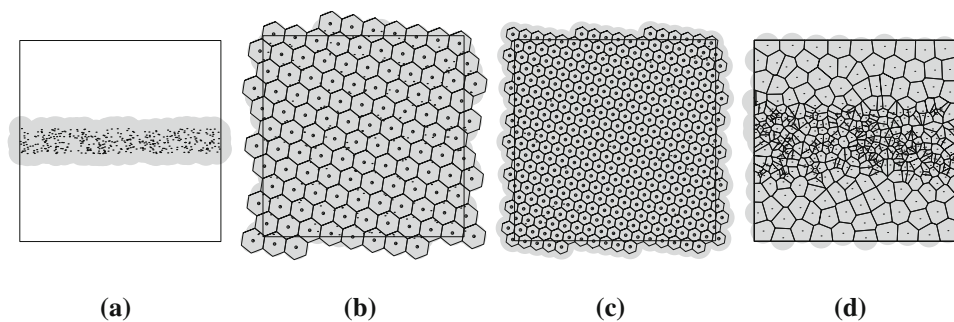


Fig. 13 Trail initial deployment (a) and comparison among PP1 (b), PP2 (c) and VOR_{MM} (d)

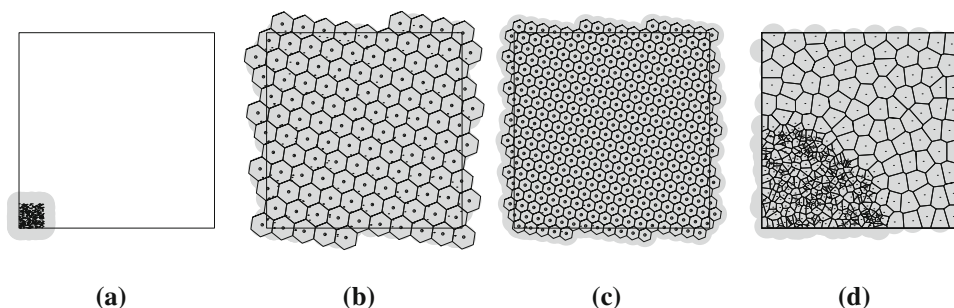


Fig. 14 Safe location initial deployment (a) and comparison among PP1 (b), PP2 (c) and VOR_{MM} (d)

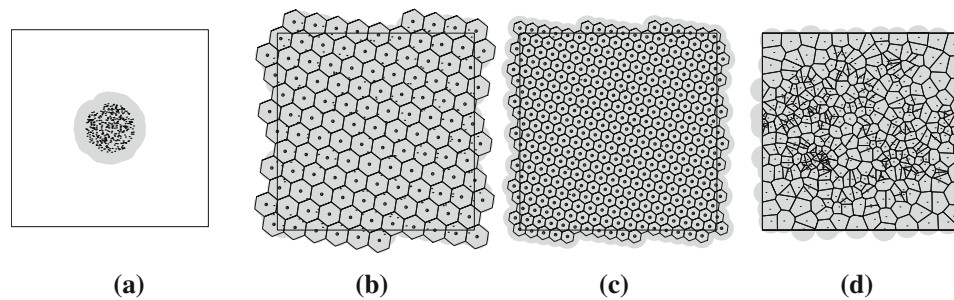


Fig. 15 Central initial deployment (a) and comparison among PP1 (b), PP2 (c) and VOR_{MM} (d)

We compare the behavior of the three algorithms with respect to several performance objectives: energy consumption, coverage uniformity, termination and coverage completion time.

All the figures from 16 to 20 contain three plots each. Plot (a) describes the performance obtained when starting from the trail initial deployment, plot (b) refers to the case in which sensors are initially deployed in a safe corner while plot (c) is related to the case of a dense initial deployment in the center of the AoI. For a better readability, we adopt different scales of the vertical axis for the three scenarios.

5.2.1 Coverage uniformity

The three algorithms give different importance to the uniformity of the coverage. Indeed, Push & Pull aims at making the coverage as uniform as possible.

In particular, PP1 builds a coarse grained grid, then it tries to uniform the coverage only on the basis of a local satisfaction of the Moving Condition.

Instead PP2 constructs a fine grained grid by setting the hexagon side at the minimum length which guarantees the full coverage of the AoI, thus making sensors traverse longer distances than other solutions.

On the contrary, VOR_{MM} aims at covering the AoI regardless of the uniformity of the final coverage, and sensors stop moving when the AoI is fully covered.

In order to evaluate the coverage uniformity, we compute the coverage density as the number of sensors covering the points of a squared mesh with side 1 m.

Figure 16 shows the standard deviation of the coverage density. Notice that we do not show the average coverage density because it is not significant, since it only depends on the number of available sensors.

The standard deviation of the coverage density achieved by PP1 and PP2 is smaller than the one obtained by VOR_{MM} . In particular, VOR_{MM} terminates as soon as the AoI is completely covered, without uniforming the density of the sensor deployment, while PP1 and PP2 keep on moving until they uniform the coverage.

This result is particularly important as a uniformly redundant sensor placement provides self-healing and fault tolerance capabilities. In the case of PP1, the presence of quite uniformly distributed slaves ensures the self-healing capability of the deployment, while for what concerns PP2, the guaranteed continuous k -coverage gives tolerance up to $(k - 1)$ faults.

5.2.2 Energy consumption

We show an analysis of the energy consumption of the three algorithms in terms of average traversed distance per sensor and average number of starting/braking actions. Finally we give an overall evaluation which also comprises the communication costs.

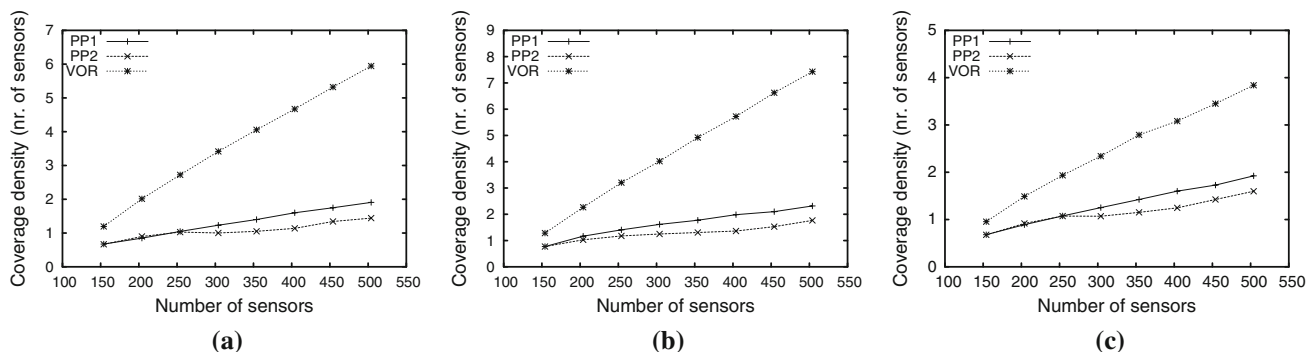


Fig. 16 Coverage density with trail (a), safe location (b) and central (c) initial deployment

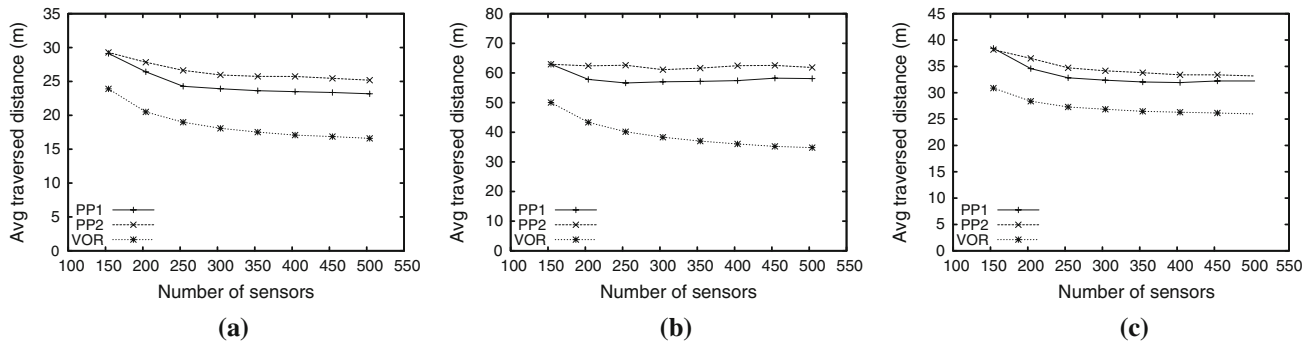


Fig. 17 Average traversed distance with trail (a), safe location (b) and central (c) initial deployment

5.2.2.1 Average traversed distance per sensor The different weight that the three algorithms give to the uniformity objective is reflected in the different trends of the average traversed distance shown in Fig. 17.

The average traversed distance of VOR_{MM} decreases with the number of sensors. This is due to the fact that more and more sensors maintain their initial positions when no coverage holes are detected. On the contrary, in both modes of Push & Pull all sensors contribute to realize a quite uniform coverage, hence the average traversed distance becomes approximately constant for large numbers of sensors. This implies that VOR_{MM} spends less energy in movements than Push & Pull at the expense of the uniformity of the final coverage, in all the considered settings of the initial deployment.

5.2.2.2 Average number of starting/braking actions per sensor We now consider the number of starting/braking actions as they require a high energy consumption [9]. Figure 18 highlights that, when the number of sensors is relatively small, VOR_{MM} performs a number of starting/braking actions higher than PP1 and PP2. On the contrary, when the number of sensors increases, VOR_{MM} apparently performs better, showing a rapid decrease of the number of starting/braking actions. This is due to the presence of a growing fraction of sensors which does not move at all, generating a final non uniform coverage as well as a high energy imbalance among sensors. The most critical

scenario for the VOR_{MM} algorithm is the safe location initial deployment (notice the different vertical scales in Fig. 18).

5.2.2.3 Average energy consumption We now analyze the overall energy consumption of the three algorithms. We utilize a unified energy consumption metric obtained as the sum of the contributions given by movements, starting/braking actions and communications. The energy spent by sensors for communications and movements is expressed in energy units. The reception of one message corresponds to one energy unit, a single transmission costs the same as 1.125 receptions [21], a 1 meter movement costs the same as 300 transmissions [9] and a starting/braking action costs the same as 1 meter movement [9].

Figure 19 shows the energy consumption of PP1, PP2 and VOR_{MM} in the three considered scenarios.

PP1 presents a stable energy consumption even when the number of sensors varies significantly. Indeed, although only a fixed number of them are snapped, all sensors are involved in the push and pull activities, thus improving the coverage density and uniforming the energy consumption.

PP2 instead, shows that the consumed energy increases as the number of sensors grows. Indeed, the more numerous are the sensors, the finer is the grid adopted by PP2. Therefore, in order to reach their destination, the slaves traverse more hexagons, and are involved in a higher number of push activities than in the case of PP1. This

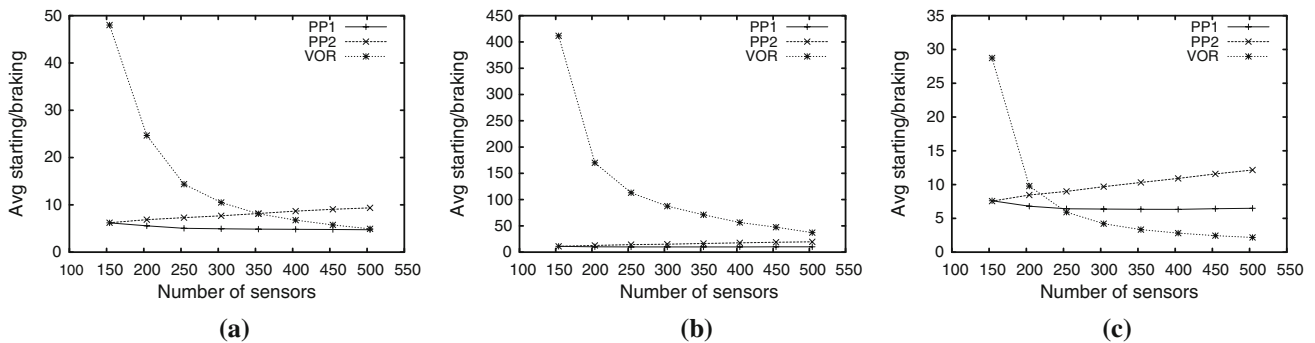


Fig. 18 Average number of starting/braking with trail (a), safe location (b) and central (c) initial deployment

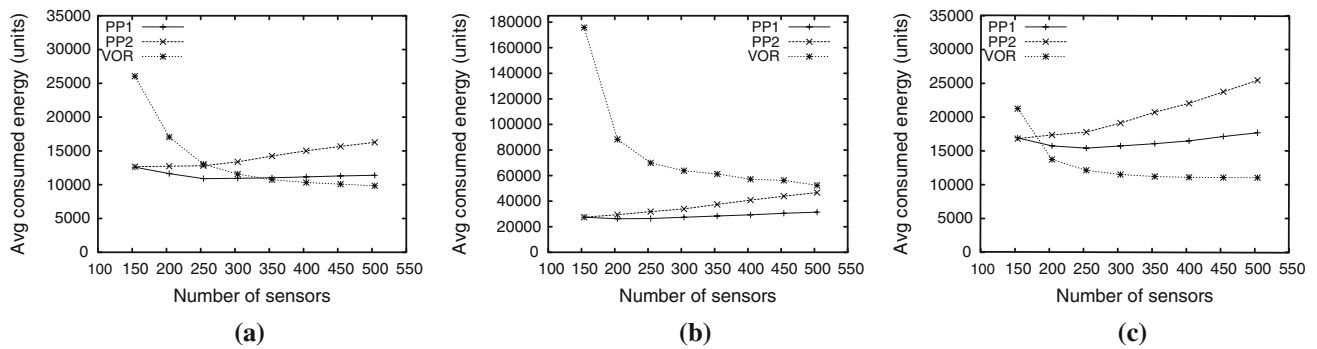


Fig. 19 Average energy consumption with trail (a), safe location (b) and central (c) initial deployment

increases the number of starting/braking actions as shown in Fig. 18 and also increases the consumed energy consequently.

VOR_{MM} consumes more energy than PP1 and PP2, when the number of sensors is close to the tight value. Although sensors do not traverse long distances (as shown in Fig. 17), the limit on the maximum moving distance per round required by VOR_{MM} increases the number of starting/braking actions (see Fig. 18), thus resulting in a high energy consumption. This effect is particularly evident in the case of the safe location scenario shown in Fig. 19(b).

The average energy consumption of VOR_{MM} decreases when increasing the number of sensors. Notice that this is not due to a better behavior of the algorithm but to the fact that a greater and greater fraction of sensors do not move at all. This implies that a considerable number of sensors consume a large amount of energy to move from overcrowded regions toward uncovered areas. As soon as all the coverage holes are eliminated, VOR_{MM} stops, leaving some zones with very low density coverage. These zones are prone to the occurrence of coverage holes in case of failures, as the sensor density is very scarce and the only sensors located in proximity have already consumed much energy during the network deployment.

Although PP2 consumes more energy when the number of the available sensors grows, it guarantees a more uniform coverage with respect to VOR_{MM} and PP1. Moreover,

the regularity of the final deployment enables the use of topology control algorithms [17] that permit a selective sensor activation, saving energy during the operative phase which follows the deployment.

5.2.3 Coverage completion and termination time

Figure 20 shows the coverage and termination time for the three algorithms. Notice that for VOR_{MM} the termination and coverage completion times coincide, while for Push & Pull some more movements are still executed even after the coverage completion.

In the three considered scenarios, if the number of sensors available is close to the minimum needed to cover the AoI, VOR_{MM} requires a very long time to complete the coverage, while Push & Pull terminates much earlier. When the number of available sensors grows, VOR_{MM} has a shorter termination time, which instead remains stable under PP1. On the contrary, the termination time of PP2 grows when the number of available sensors increases. In particular, VOR_{MM} generally requires more time than PP1 to achieve its final coverage. Only in the case of the central initial deployment, and for a high number of available sensors ($N > 320$) VOR_{MM} terminates in a shorter time if compared with PP2 (see Fig. 20c). This is due to the fact that the termination time of PP2 is delayed by the numerous hole triggers generated by the pull activity.

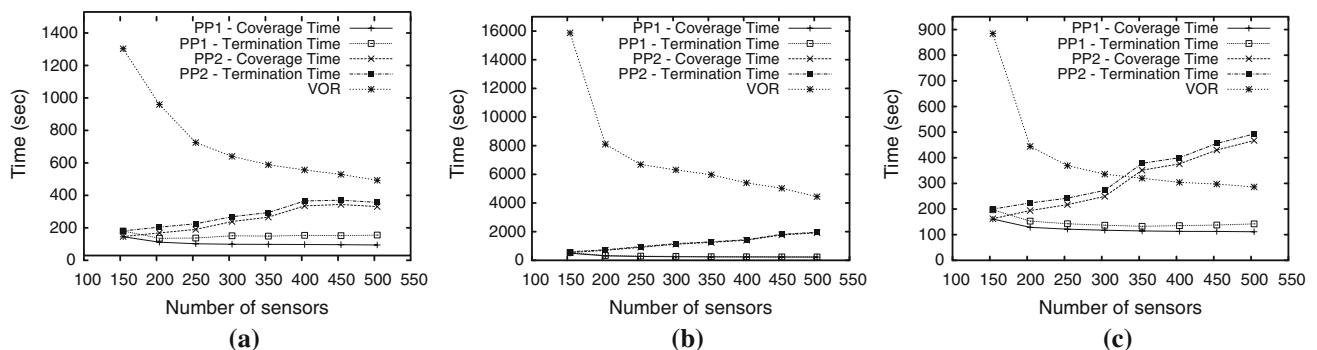


Fig. 20 Termination and coverage time with trail (a), safe location (b) and central (c) initial deployment

It is worth noting that as already discussed, the safe location deployment, constitutes a critical scenario for VOR_{MM} as this algorithm works at its best for more uniform initial sensor distributions. Indeed, Fig. 20(b) shows that VOR_{MM} requires much more time than in the other sets of experiments, (a) and (c), to achieve its final deployment (16000 s in the case of safe location vs. 1400 s in the case of trail, and 900 s in the case of central initial deployment).

6 Related work

There is an impressively growing interest in self-managing systems, starting from several industrial initiatives from IBM [22], Hewlett Packard [23] and Microsoft [24]. Various approaches have been proposed to self-deploy mobile sensors although few of them can be actually considered autonomic. The majority of these works are either based on the virtual force approach (VFA) or on computational geometry techniques.

The virtual force approach (VFA) [2–4] models the interactions among sensors as a combination of attractive and repulsive forces. This approach requires the definition of thresholds to determine the magnitude of the force one sensor exerts on another. As shown in [4], the VFA presents oscillatory sensor behavior. This problem is addressed by defining further arbitrary thresholds as stopping conditions. The tuning of such thresholds is laborious and relies on an off-line configuration. In addition, it influences the resulting deployment, the overall energy consumption and the convergence rate. Moreover, this approach does not guarantee the coverage in presence of narrows. A variation of the VFA is presented in [5] where the introduction of two virtual forces guarantees better uniformity by providing at least K neighbors to each sensor. Other approaches are inspired by physics as well, such as [6, 7]. In [6] the sensors are modelled as particles of a compressible fluid and regulates their movement mimicking a diffusive behavior. In [7] two approaches that make use of gas theory to model sensor movements in presence of obstacles are proposed. However the last three approaches still suffer from oscillatory sensor behavior. The work [8] introduces a unified solution for sensor deployment and relocation which also makes use of the virtual force approach. This proposal deals with a rather different problem with respect to ours. Indeed this work is designed for an open environmental setting, namely where the target area is not determined prior to the deployment.

By contrast, the techniques based on computational geometry, model the deployment problem in terms of Voronoi diagrams or Delaunay triangulations.

The Voronoi approach (VOR_{MM}) is detailed in [9]. According to this proposal, each sensor iteratively

calculates its own Voronoi polygon, determines the existence of coverage holes and moves to a better position if necessary. In this approach the relationship between the transmission and the sensing range influences the obtained performances by either moving sensors toward already covered positions or reducing the resulting covered area. Furthermore, this approach is not designed to improve the uniformity of an already complete coverage. According to [10] each sensor makes a rough evaluation of the local density and calculates the movements needed to reach a final position that is as close as possible to the points of a hexagonal tiling. This is done by locally constructing the Delaunay triangulation determined by the current sensor placement. This approach suffers from similar limitations to the VFA and does not guarantee oscillation avoidance if proper threshold parameters are not set.

In [11] the authors analyze the problem of sensor deployment in a hybrid scenario, with both mobile and fixed sensors in the same environment. They introduce the general concept of logical movements. Instead of moving iteratively, sensors calculate their target locations based on a distributed iterative algorithm, move logically, and exchange new logical locations with their new logical neighbors. Actual movement only occurs when sensors determine their final locations, thus sparing energy by avoiding zig-zag motions at the expense of some more messaging activity.

A different approach is proposed in [12], which introduces a technique for sensor deployment for operative settings where the sensing radius is relatively large, hence coverage does not necessarily imply connectivity. These operative settings are not addressed by our paper which instead deals with the most common types of devices for which the relation between the sensing and the transmission radius is such that the achievement of a complete coverage also guarantees network connectivity.

7 Conclusions and future work

We proposed an original algorithm for mobile sensor self deployment named Push & Pull. According to our proposal, sensors autonomously coordinate their movements in order to achieve a complete and uniform coverage with moderate energy consumption. The execution of Push & Pull does not require any prior knowledge of the operating conditions nor any manual tuning of key parameters, as sensors adjust their positions on the basis of locally available information. The proposed algorithm leads to a guaranteed final static and uniform coverage, provided that there is a sufficient number of sensors. As experiments show, Push & Pull outperforms previously proposed approaches thanks to its ability to cover target areas of even

irregular shape. Mechanisms for obstacle detection and avoidance are being investigated and considered as future extensions of this work.

References

- Howard, A., Mataric, M. J., & Sukhatme, G. S. (2002). Mobile sensor network deployment using potential fields: A distributed, scalable solution to the area coverage problem. In *Proceedings of the International Symposium on Distributed Autonomous Robotics Systems, DARS*.
- Zou, Y., & Chakrabarty, K. (2003). Sensor deployment and target localization based on virtual forces. In *Proc. IEEE INFOCOM*.
- Heo, N., & Varshney, P. (2005). Energy-efficient deployment of intelligent mobile sensor networks. *IEEE Transactions on Systems, Man and Cybernetics*, 35, 78–92.
- Chen, J., Li, S., & Sun, Y. (2007). Novel deployment schemes for mobile sensor networks. *Sensors*, 7, 2907–2919.
- Poduri, S., & Sukhatme, G. S. (2004). Constrained coverage for mobile sensor networks. In *Proc. of IEEE Int'l Conf. on Robotics and Automation (ICRA)*.
- Pac, M. R., Erkmen, A. M., & Erkmen, I. (2006). Scalable self-deployment of mobile sensor networks: A fluid dynamics approach. In *Proc. of IEEE/RSJ Int'l Conf. on Intelligent Robots and Systems (IROS)*.
- Kerr, W., Spears, D., Spears, W., & Thayer, D. (2004). Two formal fluid models for multi-agent sweeping and obstacle avoidance. In *Proc. of AAMAS*.
- Garetto, M., Gribaudo, M., Chiasserini, C.-F., & Leonardi, E. (2007). A distributed sensor relocation scheme for environmental control. In *The ACM/IEEE Proc. of MASS*.
- Wang, G., Cao, G., & La Porta, T. (2006). Movement-assisted sensor deployment. *IEEE Transaction on Mobile Computing*, 6, 640–652.
- Ma, M., & Yang, Y. (2007). Adaptive triangular deployment algorithm for unattended mobile sensor networks. *IEEE Transactions on Computers*, 56, 946–958.
- Wang, G., Cao, G., & La Porta, T. (2004). Proxy-based sensor deployment for mobile sensor networks. In *IEEE International Conference on Mobile Ad-hoc and Sensor Systems (MASS)*.
- Tan, G., Jarvis, S. A., & Kermarrec, A.-M. (2008). Connectivity-guaranteed and obstacle-adaptive deployment schemes for mobile sensor networks. In *The IEEE Proc. of ICDCS*.
- Wang, G., Cao, G., La Porta, T., & Zhang, W., (2005). Sensor relocation in mobile sensor networks. In *Proc. of IEEE INFOCOM*.
- Babaoglu, O., Jelasity, M., & Montresor, A. (2005). Grassroots approach to self-management in large-scale distributed systems. In *Unconventional programming paradigms. Lecture notes in computer science* (Vol. 3566). Springer Verlag.
- Brass, P. (2007). Bounds on coverage and target detection capabilities for models of networks of mobile sensors. *ACM Transactions on Sensor Networks*, 3, 1–19.
- Bartolini, N., Massini, A., & Silvestri, S. (2008). P&p protocol: Local coordination of mobile sensors for self-deployment. <http://arxiv.org/abs/0805.1981>. Accessed 20 December 2008.
- Pattam, S., Poduri, S., & Krishnamachari, B. (2003). Energy-quality tradeoffs for target tracking in wireless sensor networks. In *Proc. of ACM International Conference on Information Processing in Sensor Networks (IPSN), Springer Lecture Notes in Computer Science* (Vol. 2634).
- Huang, C.-F., & Tseng, Y.-C. (2005). The coverage problem in a wireless sensor network. *Elsevier Mobile Networks and Applications*, 10, 519–528.
- Zhang, H., & Hou, J. (2005). Maintaining sensing coverage and connectivity in large sensor networks. *Ad Hoc & Sensor Wireless Networks*, 1(1–2), 89–124.
- Opnet Technologies Inc. <http://www.opnet.com>. Accessed 20 December 2008.
- Performance measurements of mote sensor networks. (2004). *ACM Symposium on Modeling Analysis and Simulation of Wireless and Mobile Systems (MSWiM)*.
- IBM: The vision of autonomic computing. <http://www.research.ibm.com/autonomic/manifesto>. Accessed 20 December 2008.
- Hewlett Packard: Adaptive enterprise design principles. <http://www.hp.com/hpinfo/newsroom/press/2003/030506a.html>. Accessed 20 December 2008.
- Microsoft: The drive to self-managing dynamic systems. <http://www.microsoft.com/windowserversystem/dsi/default.aspx>. Accessed 20 December 2008.

Author Biographies



Novella Bartolini graduated with honors in 1997 and received her Ph.D. in Computer Engineering in 2001 from the University of Rome, Italy. She is now assistant professor at the University of Rome. She was researcher at the Fondazione Ugo Bordoni in 1997, visiting scholar the University of Texas at Dallas in 1999–2000 and research assistant at the University of Rome ‘Tor Vergata’ in 2000–2002. She was program chair and program committee member of several international conferences. Her research interests lie in the area of wireless mobile networks and web based systems.



Tiziana Calamoneri graduated in Mathematics in 1992 and got her Ph.D. in Computer Science in 1997, at University of Rome ‘La Sapienza,’ Italy. Since 2006, she is associate professor at the Department of Computer Science, University of Rome ‘La Sapienza’ where she also was assistant professor from 2000 to 2006. Her research interests include sensor networks, parallel and sequential graph algorithms, layout of

networks topologies and optimal routing schemes, channel assignment in wireless networks.



Emanuele Guido Fusco graduated in 2004 and is currently a Ph.D. student in Computer Science at Sapienza, University of Rome, Italy. He visited Prof. A. Pelc at the Université du Québec en Outaouais. He serves as reviewer of many international conferences and journals. His research interests lie in the area of sensor networks and network algorithms.



Simone Silvestri graduated with honors in 2005 and is currently a Ph.D. student in Computer Science at Sapienza, University of Rome, Italy. He is currently a visiting scholar at the Electrical and Electronic Engineering Department, Imperial College, London. He serves as reviewer of many international conferences and journals. His research interests lie in the area of sensor networks and web based systems.



Annalisa Massini graduated in Mathematics in 1989 and got her Ph.D. in Computer Science in 1993, at University of Rome “La Sapienza,” Italy. In 1996 she became assistant professor at the Department of Computer Science, University of Rome “La Sapienza”. Since 2001 she is associate professor at the Department of Computer Science, University of Rome “La Sapienza”. Her research interests include wireless networks,

algorithms on interconnection networks, layout of networks topologies, parallel arithmetic units.